

1 **Interdecadal enhancement in the relationship between western North Pacific summer**  
2 **monsoon and sea surface temperature in the tropical central-western Pacific after the**  
3 **early 1990s**

4 Kui LIU<sup>1,2</sup>, Lian-Tong ZHOU<sup>2\*</sup>, Zhibiao WANG<sup>2</sup>, Yong LIU<sup>2</sup>

5 <sup>1</sup> *College of Geography and Tourism, Hengyang Normal University, Hengyang 421008, China*

6 <sup>2</sup> *Center of Monsoon System Research, Institute of Atmospheric Physics, Chinese Academy of Sciences,*  
7 *Beijing 100029, China*

8  
9 Submitted to *Advances in Atmospheric Sciences*

10 July 18, 2022

11  
12  
13 Corresponding author address:

14 Dr. Lian-Tong ZHOU

15 Center for Monsoon System Research

16 Institute of Atmospheric Physics

17 Chinese Academy of Sciences

18 Beijing 100029

19 China

20 E-mail: zlt@mail.iap.ac.cn

21

## ABSTRACT

22 This study reveals the interdecadal strengthening in the relationship between the  
23 western North Pacific summer monsoon (WNPSM) and tropical central-western Pacific  
24 sea surface temperature anomaly (SSTA) in summer after the early 1990s. In the first  
25 period (1979–1991, P1), the WNPSM-related precipitation anomaly and horizontal  
26 wind anomaly are presented as a analogous Pacific-Japan (PJ)-like pattern, generally  
27 considered as to be related to the Niño-3 index in the preceding winter. During a  
28 subsequent period (1994–2019, P2), the WNPSM-related precipitation anomaly  
29 presents a zonal dipole pattern, correlated significantly with the concurrent SSTA in  
30 Niño 4 and tropical western Pacific. The negative (positive) SSTA in tropical western  
31 Pacific and positive (negative) SSTA in Niño 4 area, could work together to influence  
32 the WNPSM. And the two types of anomalous SSTA configuration enhance/weaken the  
33 WNPSM by the positive/ negative phase PJ-like wave and Gill response, respectively,  
34 with an anomalous cyclone/anticyclone located in WNPSM, which shows obvious  
35 symmetry about the anomalous circulation. Specifically, the SSTA in Niño 4 exerts  
36 impacts on WNPSM by atmospheric Gill response, with stronger (weaker) WNPSM  
37 along with positive (negative) SSTA in Niño 4. And the SSTA in tropical western  
38 Pacific exerts influence on the WNPSM by PJ-like wave, with stronger (weaker)  
39 WNPSM along with negative (positive) SSTA in the tropical western Pacific. In general,  
40 SSTA in the tropical western Pacific and Niño 4 could work together to exert influence  
41 on the WNPSM, mainly concentrated in the El Niño (La Niña) developing year in P2.  
42 However, SSTA in the tropical western Pacific/ Niño 4 works alone to exert influence  
43 on WNPSM mainly in 2013,2014,2016,2017/CP La Niña developing years. The  
44 sensitive experiments also can reproduce the PJ-like wave/Gill response associated with  
45 SSTA in the tropical western Pacific/Niño 4. Therefore, the respective and synergistic  
46 impacts from Niño 4 and the tropical western Pacific on WNPSM have been revealed,  
47 which helps to acquire a better understanding about the interdecadal variation of  
48 WNPSM and associated climate influences.

49

50 **Key words:** western North Pacific summer monsoon, tropical central-western Pacific,  
51 SST, interdecadal change

52

53 <https://doi.org/10.1007/s00376-023-2200-0>

54

55 **Article Highlights:**

56 The interdecadal enhancement in the relationship between the WNPSM and tropical central-western  
57 Pacific SSTA after the early 1990s has been revealed.

58 The SSTA in tropical western Pacific exerts influence on WNPSM by PJ-like wave, and SSTA in  
59 Niño 4 exerts impact on WNPSM by Gill response.

60 The respective and synergistic impacts of the Niño 4 and tropical western Pacific on WNPSM have  
61 been confirmed by numerical experiments.

in press

## 62 1. Introduction

63 Asia summer monsoons is composed of the Indian summer monsoon (ISM), East  
64 Asian summer monsoon (EASM), and western North Pacific summer monsoon  
65 (WNPSM), considered as one of the most important climate systems for earth (Wang et  
66 al. 2000; Wang et al. 2001; Kwon et al. 2005; Lee et al. 2014). Compared to ISM and  
67 EASM, the WNPSM obtained less attentions, mainly located at  $5^{\circ}$ – $15^{\circ}$ N,  $100^{\circ}$ – $130^{\circ}$ E  
68 and  $20^{\circ}$ – $30^{\circ}$ N,  $110^{\circ}$ – $140^{\circ}$ E (Wang et al. 2001). However, a large proportion of the  
69 rainfall in Indochina Peninsula, Philippines, and south China is related with the  
70 WNPSM (Vega et al. 2020), and has large variations, which can affect agriculture and  
71 lives of millions of people (Wu and Wang 2000; Wu 2002; Chou et al. 2003). Therefore,  
72 to understand the variability of WNPSM has great socioeconomic significance.

73 The WNPSM features complex spatiotemporal variations, mainly in terms of the  
74 burst, withdrawal, and the breaks along with its northward progress. The onset date  
75 displays a high interannual variability (Vega et al. 2020), and during the period the  
76 rainfall is mainly located in the South China Sea (Wu and Wang 2000; Wang and Lin  
77 2002). In contrast, the WNPSM withdrawal presents a lower interannual variation  
78 (Vega et al. 2020), spanning from September to November (Wang and Lin 2002;  
79 Janowiak and Xie 2003; Zeng and Lu 2004). In addition, during the period of  
80 northeastward movement, WNPSM has a distinct monsoon break phenomenon. When  
81 the WNPSM passes through the Philippines and the Mariana Islands (Wu and Wang  
82 2000; Wang and Lin 2002; Zhou and Chan 2007), it presents a prominent interannual  
83 variation in either intensity or duration (Wang and Xu, 1997; Xu and Lu, 2015).

84 The diverse variations of WNPSM have different climate impact, mainly in the  
85 associated circulation, precipitation, and tropical cyclone (TC) events. The strong (weak)  
86 WNPSM connects with the enhanced (reduced) precipitation over the subtropical WNP  
87 (Chou et al. 2003), and the negative (positive) rainfall anomalies along the mei-yu/baiu  
88 front (Wang et al. 2001). Even, a suppressed WNPSM has a remote influence on  
89 reduced summer rainfall over the Great Plains of the United States (Wang et al. 2001).  
90 During the break of WNPSM, striking convection suppression and remarkable decrease  
91 of precipitation over the Northeast of WNP ( $10^{\circ}$ – $20^{\circ}$ N,  $140^{\circ}$ – $160^{\circ}$ E) happens (Xu and  
92 Lu, 2016). The WNPSM is also related to the extreme precipitation, by exerting  
93 influence on TC. The WNPSM break and WNPSM trough can influence the formation

94 location, genesis frequency, and strength of TC (Gray 1968; Wu et al. 2012; Molinari  
95 and Vollaro 2013; Zong and Wu 2015; Choi et al. 2016), by the means of supplying the  
96 associated dynamic and thermodynamic conditions (Gray 1968; Briegel and Frank 1997;  
97 Wu et al. 2012; Cao et al. 2014; Zong and Wu 2015; Zhao et al. 2019), further leading  
98 to some extreme rainfall events in associated regions.

99       The influences from WNPSM on associated weather and climate are documented,  
100 and in addition, the impacts from other factors on WNPSM are also investigated, such  
101 as from intraseasonal oscillations (ISO), the atmospheric heat source, and tropical SST,  
102 etc. ISO has a significant impact on the interannual variability of onset, break of  
103 WNPSM and atmosphere-ocean interaction associated with the western Pacific  
104 subtropical high (WPSH) (Li and Wang et al. 2005; Zhou and Chan 2005; Xu and Lu,  
105 2015; He et al. 2017; Wang and Yu, 2018; Huang et al. 2018; Wu and Wang, 2019), as  
106 well as its seasonal cycle (Wu and Wang 2000; Guan and Chan 2006). Atmospheric  
107 heat sources over the WNP (Wang et al. 2001) and the tropical Indian Ocean (Xie et al.  
108 2009), are important in the formation of the circulation pattern associated with WNPSM.  
109 Besides, Hu and Long (2020) further considered that the combined action of an  
110 atmospheric heating (cooling) over the subtropical WNP and a cooling (heating) in the  
111 tropical Indian Ocean and the midlatitudes from China to the southern Japan, plays a  
112 most important role in enhancing (weakening) WNPSM. In addition, a significant  
113 connection between WNPSM and El Niño–Southern Oscillation (ENSO) has also been  
114 investigated (Wang et al. 2001). A weak (strong) WNPSM prefers to happen during the  
115 La Niña (El Niño) developing year and a strong (weak) WNPSM tends to appear in the  
116 La Niña (El Niño) decaying year (Wang et al. 2001; Chou et al. 2003). From the 1980s  
117 on, the WNPSM obviously tends to begin later (earlier) and finish earlier (later) in a  
118 eastern Pacific (EP) El Niño (La Niña) background, and the withdrawal of WNPSM is  
119 postponed (advanced) during CP La Niña (El Niño) (Vega et al. 2020). The interdecadal  
120 variation mode of the WNPSM trough is mainly related with the Pacific decadal  
121 oscillation (PDO) and the interdecadal Pacific oscillation (IPO) in different periods in  
122 the past decades, respectively (Feng and Wu, 2021). Besides, the decadal change of  
123 WNPSM break after 2002/2003 is attributed to the differences in the evolution of SST  
124 in the warm pool region of western Pacific after 2003 (Xu and Lu, 2018). Yim et al.  
125 (2008) considered that WNPSM in the period 1979–1993 is mainly linked to the  
126 warming of SST in the Niño 3 region ( $5^{\circ}\text{S}$ – $5^{\circ}\text{N}$ ,  $150^{\circ}\text{W}$ – $90^{\circ}\text{W}$ ); but in the period

127 1994–2006 is associated with the SST warming in the Niño 4 region (5°S–5°N, 160°E–  
128 150°W).

129 In general, the previous studies mainly focus on the synoptic and interannual  
130 variability of WNPSM, and its association with different key sea region in the different  
131 situation, respectively. However, different key SST areas may work together to exert  
132 influence on the WNPSM, which has obtained few attention. The present study will  
133 conduct further exploration about this issue. We have further confirmed the result  
134 shown in Yim et al. (2008) before carrying out the research in this study. But besides  
135 the enhancement of the influence from Niño 4 region after 1994, we also find that the  
136 influence of the tropical western Pacific on WNPSM is also enhanced. Namely, the  
137 interdecadal strengthening in the relationship between WNPSM and tropical central-  
138 western Pacific after the early 1990s has been found in the study. Moreover, we also  
139 further explore when Niño 4 and tropical western Pacific work in accordance to impact  
140 on WNPSM, and when they work alone to exert influences on WNPSM.

141 In this paper, the characteristics and associated physical processes of the  
142 interdecadal change in the relationship between SSTA in the tropical central-western  
143 Pacific and WNPSM are investigated. The data and methods used in the study are  
144 described in section 2. Section 3 confirms the enhancement of the interdecadal  
145 relationship between WNPSM and SSTA in the tropical central-western Pacific after the  
146 early 1990s. Section 4 outlines how the tropical central and western SSTA influences  
147 WNPSM after the interdecadal shift of the early 1990s, respectively. Section 5 discusses  
148 when tropical western Pacific, and Niño 4 area work in coherence to influence the  
149 WNPSM, and when they work alone to exert an impact on WNPSM, respectively.  
150 Finally, conclusions and a discussion are presented in the section 6.

## 151 **2. Data and Methods**

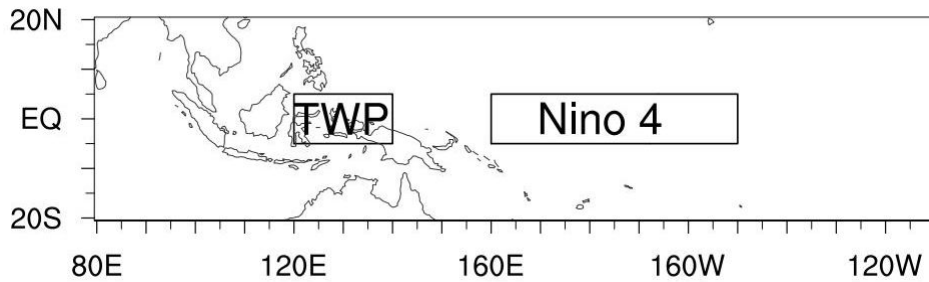
152 In this paper, JRA-55 monthly reanalysis data are applied, with  $1.25^\circ \times 1.25^\circ$   
153 horizontal resolution (Kobayashi et al. 2015). Monthly precipitation data from the  
154 Global Precipitation Project (GPCP) are adopted, with  $2.5^\circ \times 2.5^\circ$  horizontal resolution  
155 (Adler et al. 2003). Monthly average SST data (HadISST version 1.1) are obtained from  
156 the Hadley Centre, with  $1^\circ \times 1^\circ$  horizontal resolution (Rayner et al. 2003). This study  
157 focuses on the period from 1979 to 2019. The 15-year sliding correlation is applied in  
158 this study, which can extract the active time ranges of two factors acting mutually and

159 resist the disturbance of noises (Xie et al. 2016). Here, the width of the moving window  
160 (15 years) was determined considering the sample size.

161 The WNPSM index (hereafter WNPSMI) was defined as the normalized difference  
162 of 850-hPa zonal wind between the southern region ( $5^{\circ}$ – $15^{\circ}$ N,  $100^{\circ}$ – $130^{\circ}$ E) average  
163 and northern region ( $20^{\circ}$ – $30^{\circ}$ N,  $110^{\circ}$ – $140^{\circ}$ E) average, following Wang and Fan (1999)  
164 and Wang et al. (2001). Namely, the bigger WNPSMI value is, the stronger the  
165 WNPSM is. The Niño-3 index is defined as the average of SSTAs in the eastern  
166 equatorial Pacific ( $5^{\circ}$ S– $5^{\circ}$ N,  $90^{\circ}$ – $150^{\circ}$ W). Here, JJA (June, July and August) refers to  
167 the summer. In the figures, “A” and “C” indicate the anomalous anticyclone and  
168 cyclone, respectively, which are marked in Figures 5-11. We also define the tropical  
169 western Pacific index (TWPI) using SSTA averaged over  $5^{\circ}$ S– $5^{\circ}$ N,  $120^{\circ}$ – $140^{\circ}$ E, and  
170 the Niño 4 index using SSTA in  $5^{\circ}$ S– $5^{\circ}$ N,  $160^{\circ}$ E– $150^{\circ}$ W. And the normalized sequence  
171 of the subtraction between Niño 4 and TWPI is defined as the tropical central-western  
172 Pacific thermal contrast index (TCWI).

173 To confirm the relative influence of the Niño 4 and tropical western Pacific on  
174 WNPSM, we perform the numerical experiments using the Community Atmospheric  
175 Model of version 5.0, which is widely used for a variety of atmosphere- and climate-  
176 related studies and offers an ability to be configured with a variety of physical  
177 parameterization suites of varying complexity. The model is developed by the National  
178 Center for Atmospheric Research with an approximately  $1.9^{\circ} \times 2.5^{\circ}$  latitude-longitude  
179 spatial resolution and 31 vertical levels (Neale et al., 2010). We perform one control  
180 experiment and three sensitivity experiments. In all experiments, the model is integrated  
181 for 20 years. The control experiment serves as a reference for the sensitivity experiment,  
182 with climatological monthly SST for the period 1981–2010 specified in the global  
183 oceans. In the sensitivity experiments, the SST forcing is composed of climatological  
184 monthly SST and monthly idealized SST anomalies added in Niño 4 ( $5^{\circ}$ S– $5^{\circ}$ N,  $160^{\circ}$ E–  
185  $150^{\circ}$ W), marked in the right box in Fig.1, in the tropical western Pacific ( $5^{\circ}$ S– $5^{\circ}$ N,  
186  $120^{\circ}$ E– $140^{\circ}$ E), marked in the left box in Fig.1, as well as these both as shown,  
187 determined based on the statistical analyses. The specified monthly SST forcing repeats  
188 from year to year, and the largest SST anomalies are  $0.6^{\circ}$ C and  $-0.6^{\circ}$ C, respectively. In  
189 the first sensitivity experiment, positive SST anomalies are added in the central Pacific  
190 to climatological monthly SST, and the results are displayed in Fig. 6(f). In the second  
191 sensitivity experiment, negative SST anomalies are added in the western Pacific to

192 climatological monthly SST, and the results are shown in Fig. 7(f). In the third  
193 sensitivity experiment, positive and negative SST anomalies are added in the above two  
194 regions, respectively, to climatological monthly SST, shown in Fig. 9. The differences  
195 of last 16 years horizontal wind anomalies between sensitivity experiments and control  
196 experiment represent the atmospheric circulation response to the JJA SST anomalies.



197

198 **FIG. 1.** The locations to add SSTA in sensitive experiments.

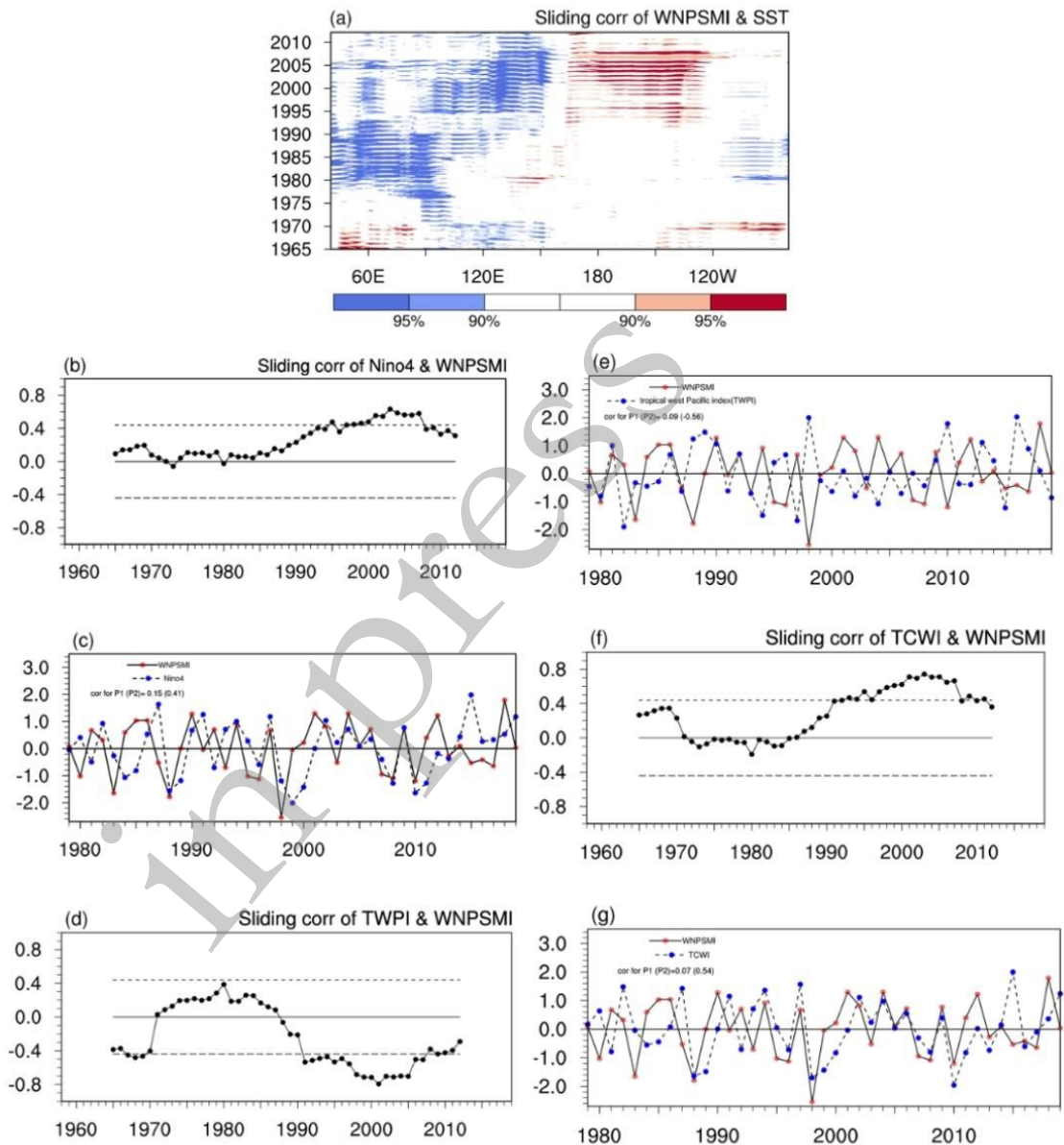
### 199 **3. Interdecadal change in the relationship between WNPSM and the tropical** 200 **central-west Pacific SST**

201 As displayed in Fig. 2a, the significant domains of correlation between WNPSM  
202 and the tropical SST, mainly concentrate in the tropical Indian Ocean prior to the 1990s,  
203 but after the 1990s, the significant areas mainly appear in the tropical central-west  
204 Pacific. It means that a strong (weak) WNPSM is accompanied by a cold (warm) SSTA  
205 in the tropical Indian Ocean before the early 1990s. Whereas, when the positive  
206 (negative) SSTA appears in the Niño 4 (5°S–5°N, 160°E–150°W) area and negative  
207 (positive) SSTA appears in the tropical west Pacific (5°S–5°N, 120°E–140°E), a strong  
208 (weak) WNPSM easily generates after the early 1990s. The key SSTA areas associated  
209 with strength of WNPSM differ greatly before and after 1990, therefore, we divide the  
210 research period into two subsection 1979–1991 (Period 1, referred to as P1) and 1994–  
211 2019 (Period 2, P2).

212 As shown in Figs. 2b, 2c, there is an obvious interdecadal change in the  
213 relationship between Niño 4 and WNPSMI, with an insignificant correlation during P1,  
214 and a significant correlation up to 0.41 ( $p > 95\%$ ) during P2. Similarly, as shown in Figs.  
215 2d, 2e, there is an obvious interdecadal change in the relationship between TWPI and  
216 WNPSMI, also with an insignificant correlation during P1, and a significant correlation  
217 up to  $-0.56$  ( $p > 99\%$ ) during P2. As shown in Figs. 2(f), (g), we define TCWI, and  
218 calculate its correlation with WNPSMI, with the correlation coefficient up to 0.54 ( $p >$

219 99%) during P2.

220 The correlation between TWPI and WNPSMI (-0.56) during P2 is more significant  
221 than that between Niño 4 and WNPSMI (0.41), and that between TCWI and WNPSMI  
222 (0.54), which implies that the SSTA in Niño 4 and TWPI do not always work in  
223 coherence, and tropical western Pacific SST may play a more important role in  
224 influencing WNPSM during P2.



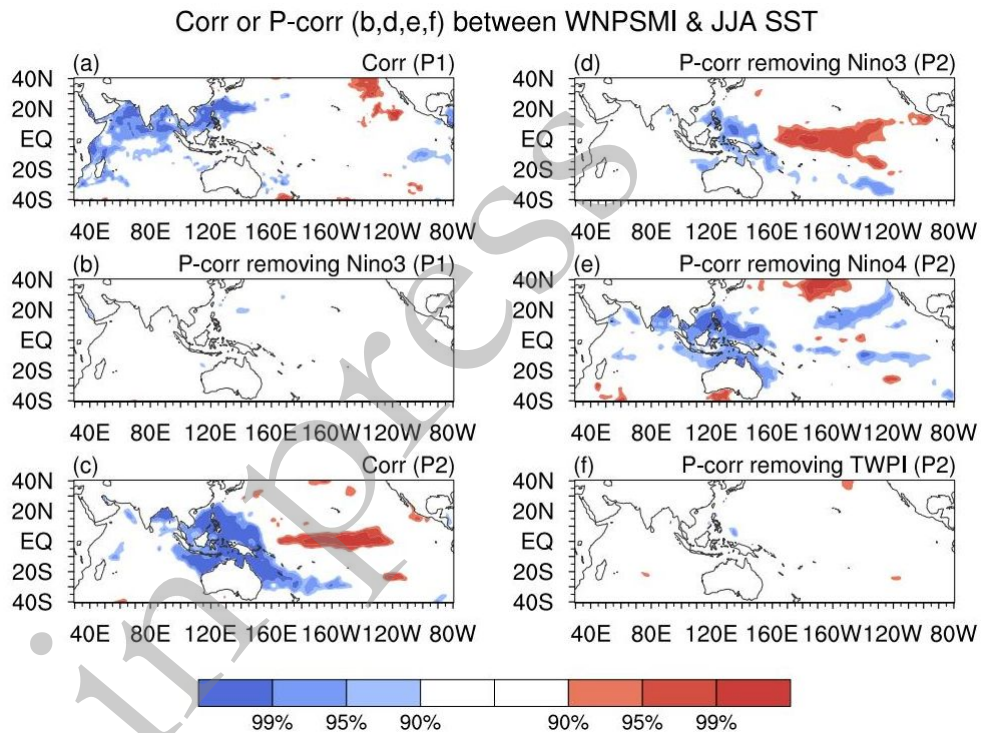
225

226 **FIG. 2.** (a) The 15-year moving correlation between WNPSMI and simultaneous JJA  
 227 SST (9.5°S–9.5°N); light/dark areas on behalf of 90%/95% confidence level. (b) The  
 228 15-year moving correlation between WNPSMI and concurrent Niño-4, and dashed lines  
 229 indicate 90% confidence level. (c) The WNPSMI index and JJA Niño-4 index, as well  
 230 as their correlation between 1979–1991 (P1) and 1994–2019 (P2). (d), (e) same as (b),  
 231 (c), but for TWPI. (f), (g) same as (b), (c), but for TCWI.

232

233 As displayed in Fig. 3a, the significant area of correlation mainly concentrates in  
 234 the tropical Indian ocean in JJA. However, when the impact of Niño 3 in the preceding  
 235 winter is detached, the correlation decreases dramatically, as presented in Fig.3b. Hence,  
 236 the WNPSM is mainly related to SSTA of Niño 3 in the preceding winter during P1,  
 237 consistent with the result obtained by Yim et al. (2008).

238



239

240 **FIG. 3.** Correlation (a) and (b) partial correlation of WNPSMI and synchronous JJA  
 241 SST, detaching impact of Niño 3 in preceding winter during P1. (c)–(d) same as (a)–(b),  
 242 but for P2, and (e), (f) same as (d), but removing the synchronous impact of Niño 4 and  
 243 TWPI, respectively. Light to dark shading indicates 90%, 95%, and 99% confidence  
 244 levels.

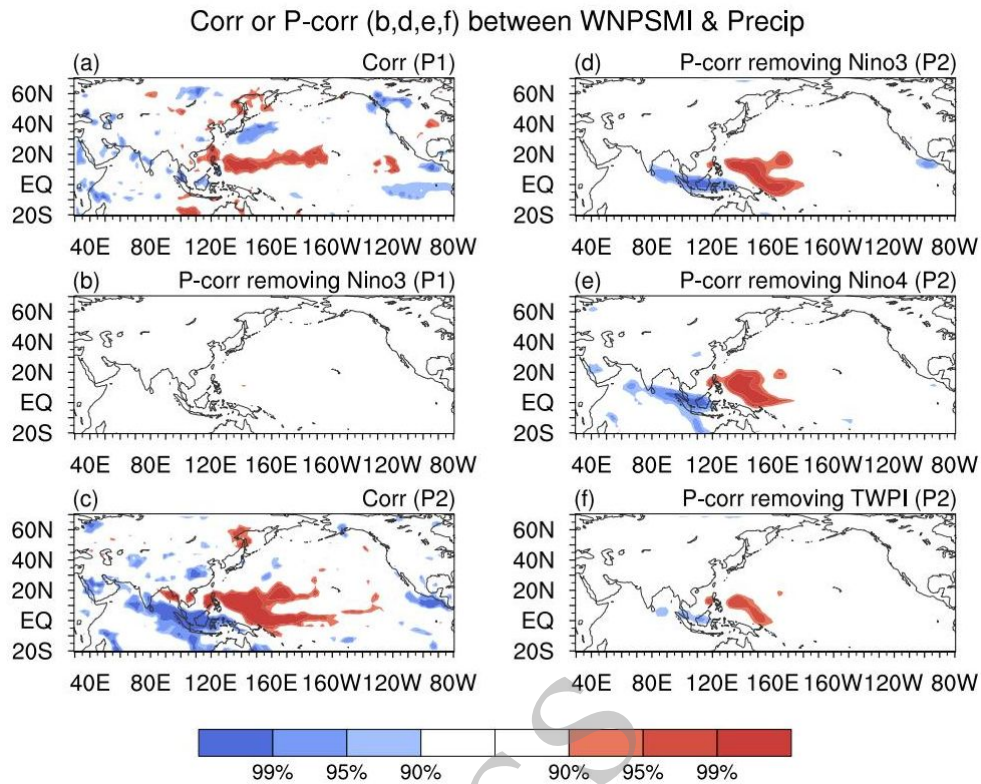
245

246 As shown in Fig. 3c, the significant region of correlation is mainly located in the  
 247 tropical west Pacific and central Pacific. However, when the influence from Niño 3 in  
 248 the preceding winter is removed (Fig. 3d), the significant correlation in the tropical  
 249 western and central Pacific still remains there, which suggests that SSTA associated

250 with WNPSMI during P2 is not governed by Niño 3 in the preceding winter, which  
251 differs greatly to that in P1. When the concurrent influence of Niño4 (Fig. 3e) is  
252 removed, the SSTA in the tropical western Pacific still remains and only the SSTA in  
253 central Pacific disappears. However, when the influence of TWPI is removed, the  
254 significance over the tropical central-west Pacific decrease dramatically (Fig. 3f), which  
255 implies that compared to Niño 4, maybe TWPI plays a more important and independent  
256 role in exerting influences on WNPSMI during P2.

257 As displayed in Fig. 4a, the most visible precipitation anomaly is a Pacific-Japan  
258 (PJ)-like pattern in JJA during P1. Nevertheless, when the impact from Niño 3 in  
259 preceding winter is removed, the areas through above 90% confidence level almost  
260 disappear (Fig. 4b), which further indicates that the relationship between WNPSMI and  
261 precipitation over western Pacific and East Asia is mainly dominated by Niño 3 during  
262 P1.

263 As displayed in Fig. 4c, the significant precipitation anomaly demonstrates a dipole  
264 pattern during P2, with negative correlation to the west of 140°E and positive  
265 correlation to the east of 140°E, which means that a strong WNPSM is accompanied by  
266 a positive rainfall anomaly in the tropical western Pacific and a negative rainfall  
267 anomaly in Marine continent. When the influence from Niño 3 in the preceding winter  
268 and concurrent Niño 4 is removed respectively, the significance dipole pattern still  
269 remains (Figs. 4d, e), which bears a similarity to the pattern shown in SSTA in Fig. 3(c),  
270 except within a smaller scope and shifting westward. Whereas, the dipole pattern  
271 weakens obviously, with the removing of the influence from TWPI (Fig. 4f), which  
272 means that the precipitation linked with WNPSM during P2, is mainly connected with  
273 both Niño 4 and TWPI, both of which obtain less modulations of Niño 3 in the  
274 preceding winter. Moreover, maybe the tropical western Pacific plays a more important  
275 role, same as the results obtained in Fig. 3.



276

277 **FIG. 4.** Same as Fig. 3 but for WNPSMI and grid GPCP precipitation.

278

279 The circulations related to WNPSMI also have different features during P1 and P2.

280 During P1, when WNPSM is strong, the anomaly of horizontal wind related to WNPSM

281 exhibits a positive-phase PJ-like pattern, with anomalous cyclones existing in  $0^{\circ}$ – $30^{\circ}$ N

282 and mid–high latitudes ( $45^{\circ}$ – $60^{\circ}$ N) and an anomalous anticyclone in between ( $30^{\circ}$ –

283  $45^{\circ}$ N) at 850-hPa level (Fig. 5a), which parallels the pattern displayed in Fig. 4(a). A

284 similar tripolar pattern also exists in the horizontal wind of 200-hPa, albeit with

285 anomalous cyclone near the equator tilting northward, a stronger middle polarity and a

286 weaker cyclone in northernmost polarity (Fig. 5b). During P1, the PJ-like pattern

287 features an equivalent barotropic structure in the lower and upper troposphere.

288 Furthermore, the PJ-like pattern could also be distinguished in the 500-hPa geopotential

289 height, with the significant area only centered in the polarity near the equator, and the

290 significant area in 2-m air temperature passing through the 95% confidence level, only

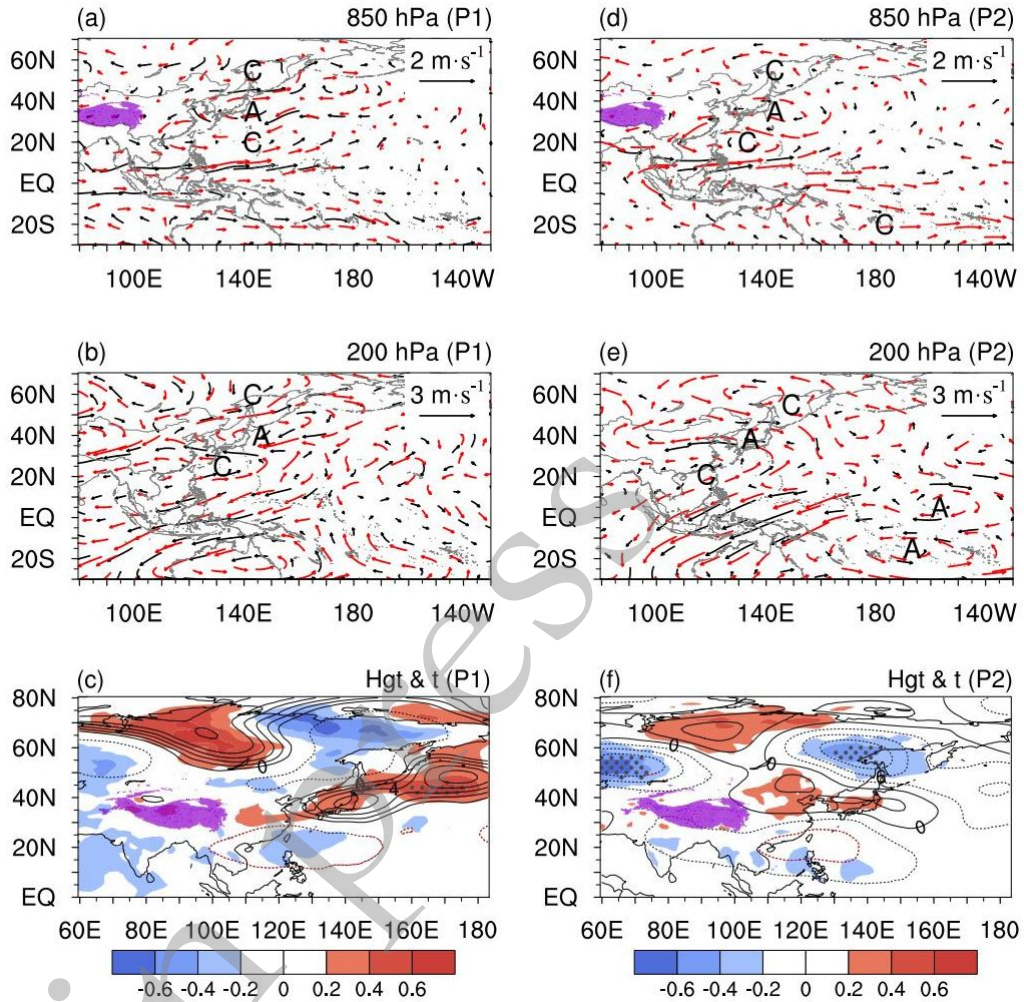
291 concentrated in the middle polarity (Fig. 5c).

292 During P1, the correlation is 0.88 between WNPSMI and PJ index, which is

293 defined as the first principal component of the EOF (Empirical orthogonal function

294 decomposition) analysis of 850-hPa vorticity field over ( $0^{\circ}$ – $60^{\circ}$ N,  $100^{\circ}$ – $160^{\circ}$ E) based

295 on Kosaka and Nakamura (2010). When the impact of Niño 3 in the preceding winter is  
 296 detached (Fig. omitted), the PJ pattern would vanish, similar to Fig. 4b. Therefore,  
 297 during P1, the anomalous circulation related to WNPSMI, mainly present a tripole  
 298 pattern, which is governed by Niño 3 in the preceding winter.



299

300 **FIG. 5.** Regression map of (a) 850 hPa horizontal wind (unit:  $\text{m s}^{-1}$ ), (b) 200 hPa  
 301 horizontal wind (unit:  $\text{m s}^{-1}$ ), and (c) 500 hPa geopotential height (unit: gpm) and 2 m  
 302 temperature (unit:  $^{\circ}\text{C}$ ) on WNPSMI during P1. (d)–(f) same as (a)–(c), but for P2. Red  
 303 vectors, dots, and red contours indicate the 95% confidence level, respectively. Violet  
 304 shading represents the Tibetan Plateau.

305

306 In contrast, the circulation anomalies associated with WNPSMI differ to some  
 307 extent during P2. The anomalous wind presents a positive PJ-like pattern in 850-hPa,  
 308 with an anomalous cyclone to the south of equator (Fig. 5d), but in 200-hPa, the  
 309 positive PJ-like pattern also appears, with two centers in the northernmost polarity and  
 310 more narrow middle polarity, also with an anomalous anticyclone to the both sides of  
 311 equator (Fig. 5e). The circulation anomalies to the both sides of equator presents a Gill

312 response-like pattern (Figs. 5d, 5e). However, during P2, the tripole pattern also can be  
313 discerned in terms of the 500-hPa geopotential height anomaly, while the northernmost  
314 polarity in the 2-m temperature anomaly is more significant (Fig. 5f), which is different  
315 to that in P1. In addition, as shown in Fig. 5f, the anomalous circulation in 500-hPa  
316 geopotential height between 40°–80°N seem to be a British-Baikal Corridor-like (BBC-  
317 like) wave, with a polarity in 60°–80°E, 90°–120°E, 130°–150°E, respectively (Xu et al.,  
318 2019).

319 Based on the above analyses, it could be found that the correlation between  
320 WNPSM and tropical Pacific SST underwent an conspicuous interdecadal shift around  
321 the early 1990s, with WNPSM significantly linked to tropical Indian Ocean, governed  
322 by the influence of Niño 3 in the preceding winter during P1, and significantly  
323 connected with the tropical western Pacific and Niño 4 SSTA, both of which obtain less  
324 influence of Niño 3 in the preceding winter during P2. Maybe, the SSTA in the tropical  
325 western Pacific plays a more important role during P2, compared with Niño 4, identical  
326 to the results obtained in rainfall and circulation associated with WNPSM.

#### 327 **4. The respective influence of SST in Niño 4 and tropical west Pacific on WNPSM** 328 **during P2**

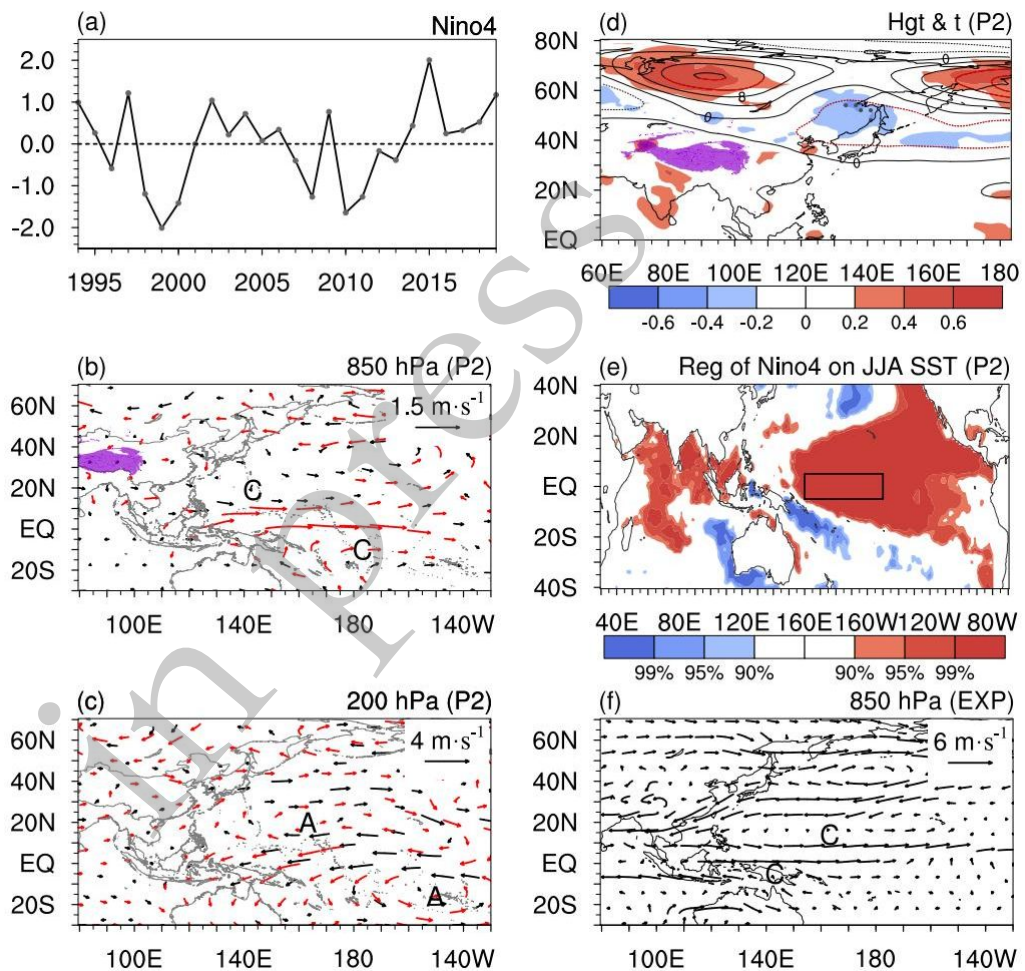
329 Many studies have revealed that the WNPSM is closely linked to El Niño -  
330 Southern Oscillation (ENSO) (Fu and Ye 1988; Zhang et al. 1996; Wu and Wang 2000).  
331 Therefore, the relationship between WNPSM and Niño 3 in the the previous winter  
332 have not been further study in this paper. This paper mainly focus on the investigation  
333 of the relationship between WNPSM and SSTA in the tropical central-western Pacific  
334 on WNPSM during P2.

335 From the analyses in section 3, we can find that both Niño 4 and tropical western  
336 Pacific have impacts on WNPSM during P2. When the influence of Niño 4 is removed,  
337 the anomalies associated with tropical western Pacific still exist, and in addition, the  
338 correlation coefficient between Niño 4 and TWPI is only –0.42 during P2, which both  
339 implies that maybe SSTA over Niño 4 and tropical western Pacific do not always work  
340 in coherence on WNPSM. Although the previous studies mainly focus the impact from  
341 Niño 4 on WNPSM after 1994 year (i.e., Yim et al. 2008). Now, it is necessary to  
342 explore the respective influence from Niño 4 and tropical Western Pacific on WNPSM

343 during P2.

#### 344 4.1 The influence of Niño 4 on WNPSM

345 As shown in Fig. 6b, when positive SSTA is located in Niño 4 area and the signals  
346 associated with TWPI are removed, an anomalous cyclone is excited in western North  
347 Pacific (WNP), accompanied by a strong WNPSM. But the tripole pattern circulation  
348 anomaly associated with WNPSM cannot be reappeared well (Figs. 6b, c), compared to  
349 Figs. 5d, 5e, respectively. In terms of the 500-hPa geopotential height anomaly and 2-m  
350 temperature anomaly in Fig. 6d, the PJ-like wave also do not appear, but the BBC-like  
351 wave still exist along  $60^{\circ}$ – $80^{\circ}$ N, similar to that in Fig. 5f.



352

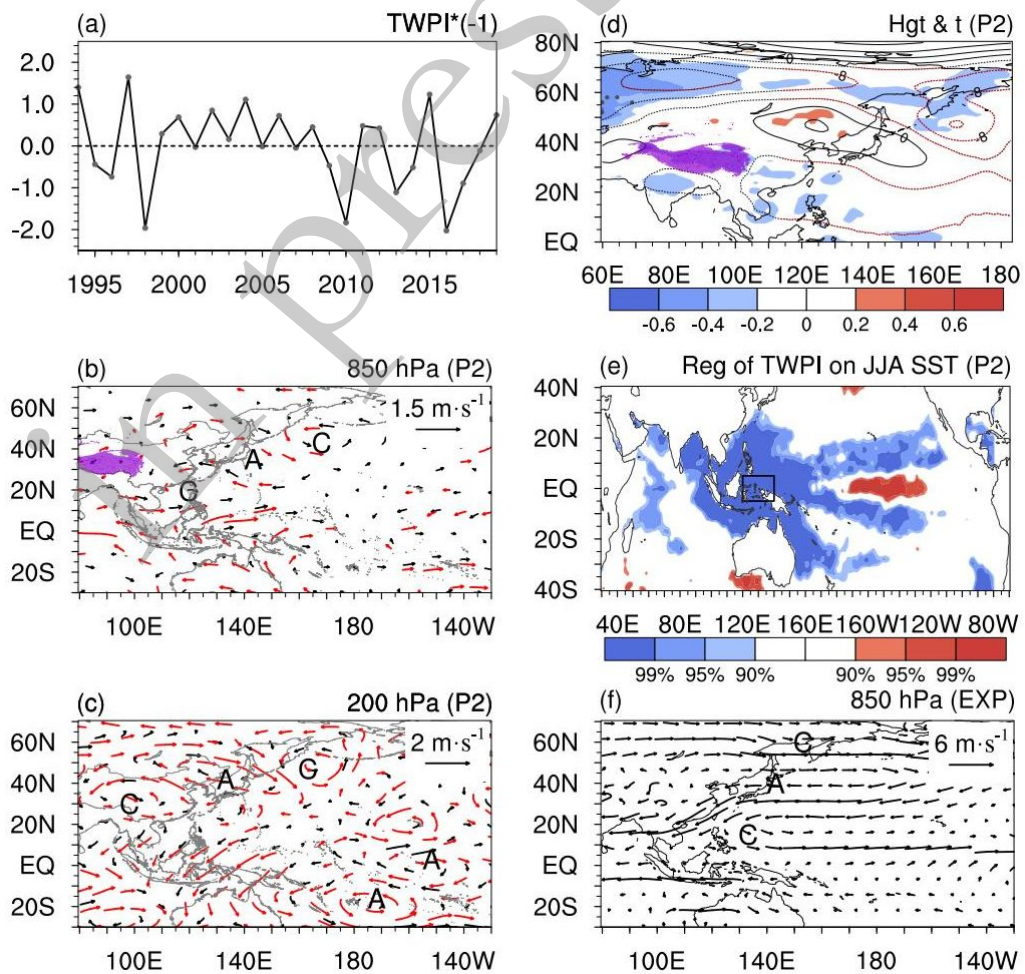
353 **FIG. 6.** (a) Normalized Niño 4 index during P2. Its regression on (b) 850-hPa  
354 horizontal wind (unit:  $\text{m s}^{-1}$ ), (c) 200-hPa horizontal wind (unit:  $\text{m s}^{-1}$ ), (d) 500-hPa  
355 geopotential height (unit:  $\text{gpm}$ ) and 2-m temperature (unit:  $^{\circ}\text{C}$ ), (e) JJA SST during P2,  
356 after removing the signals of TWPI. (f) The sensitive experiment minus the control  
357 experiment, the SST anomaly is added in the rectangle in (e), detailed description  
358 shown in section 2. Red vectors, red contours, and dots represent the 95% confidence  
359 level in Figs. (b)-(d). Light to dark shadings represent 90%, 95%, and 99% confidence  
360 level. Violet shading highlights the Tibetan Plateau.

361

362 As shown in Figs. 6b and 6c, an anomalous cyclone generates in the south and  
363 north sides to the equator at the level of 850 hPa, which transforms into anomalous  
364 anticyclonic circulation at 200 hPa (Fig. 6c). The configurations of the anomalous  
365 circulation in lower and higher layers show that positive SSTA induces the response of  
366 the atmosphere Gill type and the anomalous cyclone at the north side to the equator in  
367 850 hPa can enhance the WNPSM, which is consistent with circulation anomalies in  
368 20°S–20°N displayed in Figs. 5d, 5e. When the positive SSTA is added in the Niño 4  
369 area, marked by rectangle in Fig. 6e, the sensitive experiment also can reproduce the  
370 Gill response (Fig. 6f), same as the statistical results in Fig. 6b. So, the anomalous  
371 cyclone in WNP associated with Gill response may be an important factor of Niño 4  
372 exerting influences on WNPSM.

#### 373 4.2 The influence of tropical west Pacific SST on WNPSM

374



375

376 **FIG. 7.** Same as Fig. 6, but for TWPI.

377

378 As shown in Fig. 7b, when the negative SSTA appears in tropical western Pacific  
379 and the signals related to Niño 4 are removed, an anomalous positive-phase PJ-like  
380 pattern can be reproduced, very similar to that in Fig. 5d, and the polarity over WNP  
381 helps to enhance the WNPSM. The anomalous circulation displayed in Fig.7c also can  
382 reproduce that shown in Fig. 5e. In terms of the 500-hPa geopotential height anomaly  
383 and 2-m temperature anomaly, the circulation anomaly in Fig. 5f can also be reproduced  
384 well, only with a weaker temperature anomaly and stronger geopotential height  
385 anomaly (Fig. 7d). The negative SSTA in the tropical western Pacific excites influence  
386 on WNPSM by the positive PJ-like circulation anomaly, which can be verified in 7f,  
387 because the different between the sensitive and control experiment can also reproduce  
388 the statistical results, also displaying a PJ-like pattern. Although the Gill response-like  
389 pattern also exists in 20°S–20°N displayed in Fig. 7c, maybe this is a signal associated  
390 with Niño 4 related to TWPI, displayed in Fig. 7e.

391 Therefore, we initially believe that the SSTA in Niño 4 (tropical western Pacific)  
392 generate influences on WNPSM by Gill response (PJ-like wave).

### 393 **5. The different influences of Niño 4 and TWPI working in coherence and out of** 394 **coherence**

395 In section 4, the impacts from both Niño 4 and tropical western Pacific SSTA on  
396 WNPSM have been analyzed. Through the comparison among Figs. 2c, 2e, 2g, and Figs.  
397 3c, 3e, 3f, it can be found that the SSTA related-to WNPSM, located in Niño 4 and  
398 tropical western Pacific do not always work in accordance, namely not always with a  
399 significant negative (positive) SSTA in the tropical Western Pacific and positive  
400 (negative) SSTA in Niño 4 area. Now, it is necessary to further analyze when both work  
401 in coherence, and when the tropical western Pacific SSTA and Niño 4 area work alone  
402 to exert influence on WNPSM, respectively.

403

404 **Table 1.** The six combinations of years with different anomalies of TWPI and Niño 4,  
405 positive (negative) anomalies means beyond (below) the (minus) 0.5 standard deviation.

406

---

Types	Years
-------	-------

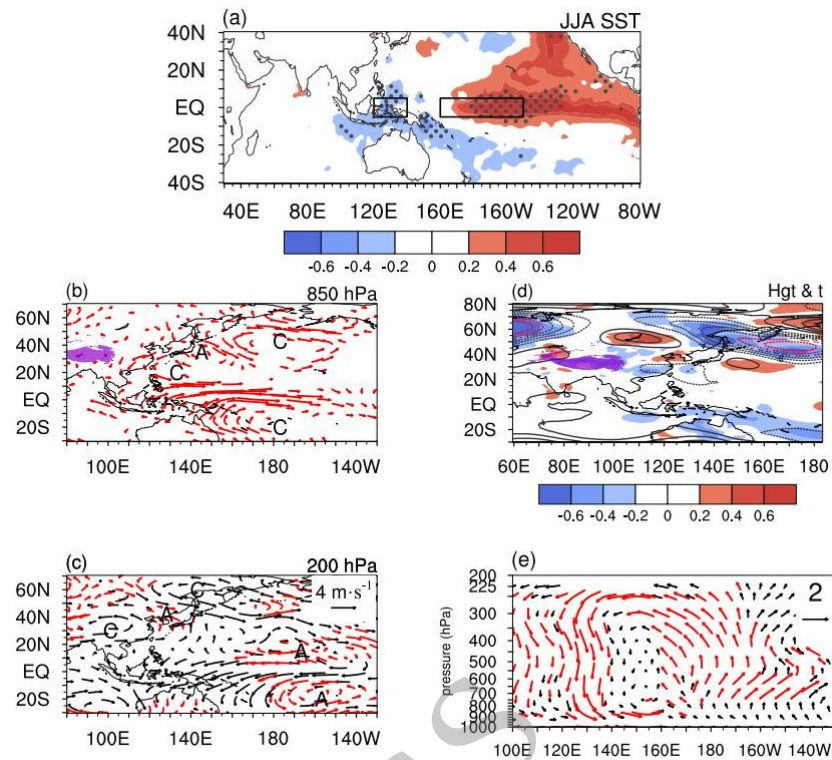
---

Negative&Positive	1994, 1997, 2002, 2004, 2015, 2019
Positive&Negative	1996, 1998, 2010
Negative&Normal	No
Positive&Normal	2013, 2014, 2016, 2017
Normal&Negative	1999, 2008, 2011
Normal&Positive	2009, 2018

407

408 As shown in Table 1, we define the year with a value (below) beyond (minus) 0.5  
409 standard deviation as (negative) positive anomaly year for TWPI and Niño 4 series,  
410 respectively. Because the SSTAs in Niño 4 and tropical western Pacific always present  
411 a dipole pattern in climatologically mean, so have no need to study “Negative &  
412 Negative”, “Positive & Positive” and “Normal & Normal” types of SSTA of TWPI and  
413 Niño 4. The necessary combinations are displayed in Table 1. During the years of 1994,  
414 1997, 2002, 2004, 2015 and 2019, the negative SSTA in the tropical Western Pacific  
415 and positive SSTA in Niño 4 area, could work in accordance to influence WNPSM;  
416 during the years of 1996, 1998 and 2010, the positive SSTA in the tropical Western  
417 Pacific and negative SSTA in Niño 4 area, also could work in accordance to influence  
418 WNPSM. During the years of 2013, 2014, 2016, and 2017, the positive SSTA anomaly  
419 in tropical western Pacific can work alone to influence WNPSM; during the years of  
420 1999, 2008, and 2011, the negative SSTA anomaly in Niño 4 area could work alone to  
421 exert impacts on WNPSM. Due to no or too few samples, the types of “Negative &  
422 Normal” and “Normal & Positive” are not discussed.

423 Based on 1994, 1997, 2002, 2004, 2015, and 2019 years, we conduct the composite  
424 analyses of SST and horizontal wind fields to explore the combination effect of the  
425 negative SSTA in the tropical Western Pacific and positive SSTA in the Niño 4 area on  
426 WNPSM (Fig. 8). As shown in Fig. 8a, it is reproduced that SSTA is positive in Niño 4  
427 area, but negative in the tropical western Pacific during 1994, 1997, 2002, 2004, 2015,  
428 and 2019 years.



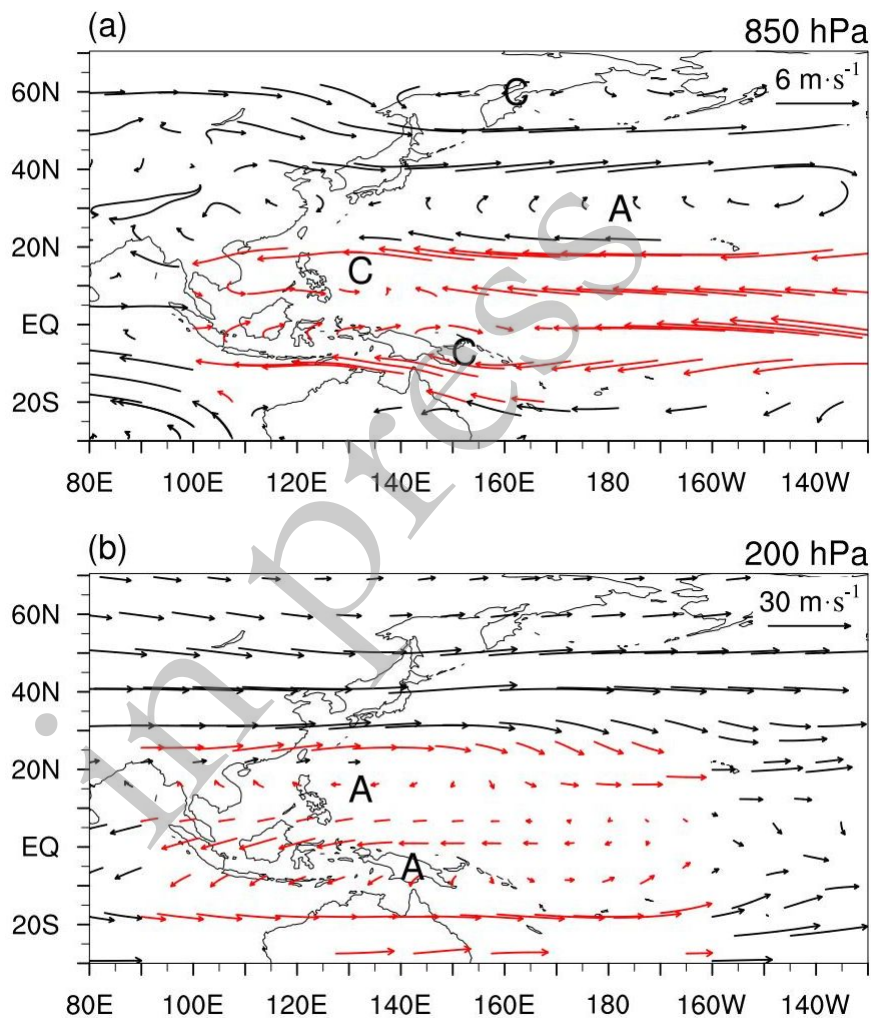
429

430 **FIG. 8.** The composite analyses of (a) SSTA, (b) 850-hPa horizontal wind (unit:  $\text{m s}^{-1}$ ), (c)  
 431 200-hPa horizontal wind (unit:  $\text{m s}^{-1}$ ), (d) 500-hPa geopotential height (unit: gpm) and  
 432 2-m temperature (unit:  $^{\circ}\text{C}$ ), (e) u and omega (multiplied by -30) based on 1994, 1997,  
 433 2002, 2004, 2015 and 2019 years. Red vectors, red contours, and dots represent the 95%  
 434 confidence level. Light to dark shadings represent 90%, 95%, and 99% confidence level.  
 435 Violet shading highlights the Tibetan Plateau.

436  
 437

438 The wind anomalies in Figs. 8b, 8c bear a great resemblance with those displayed  
 439 in Figs. 5d, 5e, respectively, which are also more similar to Figs. 7b, 7c, compared to  
 440 those displayed in Figs. 6b, 6c. In terms of the 500-hPa geopotential height anomaly and  
 441 2-m temperature anomaly, the circulation anomaly in Fig. 8d is less similar to that in  
 442 Fig. 5f, with weaker significance in temperature anomaly and stronger geopotential  
 443 height anomaly in the northernmost polarity of PJ-like pattern. From the circulation  
 444 anomalies in Figs. 8b, 8c, both the positive phase PJ-like pattern and Gill response can  
 445 be discerned. The anomalous years 1994, 1997, 2002, 2004, and 2015 are all El Niño  
 446 developing year, except for 2019 year, based on that the SSTA must be less (greater) –  
 447  $0.5^{\circ}\text{C}$  ( $0.5^{\circ}\text{C}$ ) lasting 6 months including June, July, and August. So, during the El Niño  
 448 developing year in P2, the SSTA is positive in Niño 4 and negative in tropical Western  
 449 Pacific, both of which can work in coherence to influence WNPSM by atmospheric Gill

450 response connected with SSTA in Niño 4 and anomalous PJ-like circulation associate  
 451 with western tropical Pacific. As shown in Fig. 8e, there exists an anomalous anti-  
 452 Walker circulation between the Niño 4 area and tropical western Pacific, help to  
 453 maintain the negative SSTA in tropical Western Pacific and positive SSTA in Niño 4  
 454 area. As displayed in Fig. 9, the statistical analyses also can be reproduced by the  
 455 sensitive experiment when the SSTAs are added in the tropical Western Pacific and  
 456 Niño 4 area, marked in Fig. 8a. The PJ-like pattern and the Gill response also can be  
 457 approximately reproduced in 850 hPa (Fig. 9a), and only the Gill response can be  
 458 reproduced in 200 hPa (Fig. 9b).

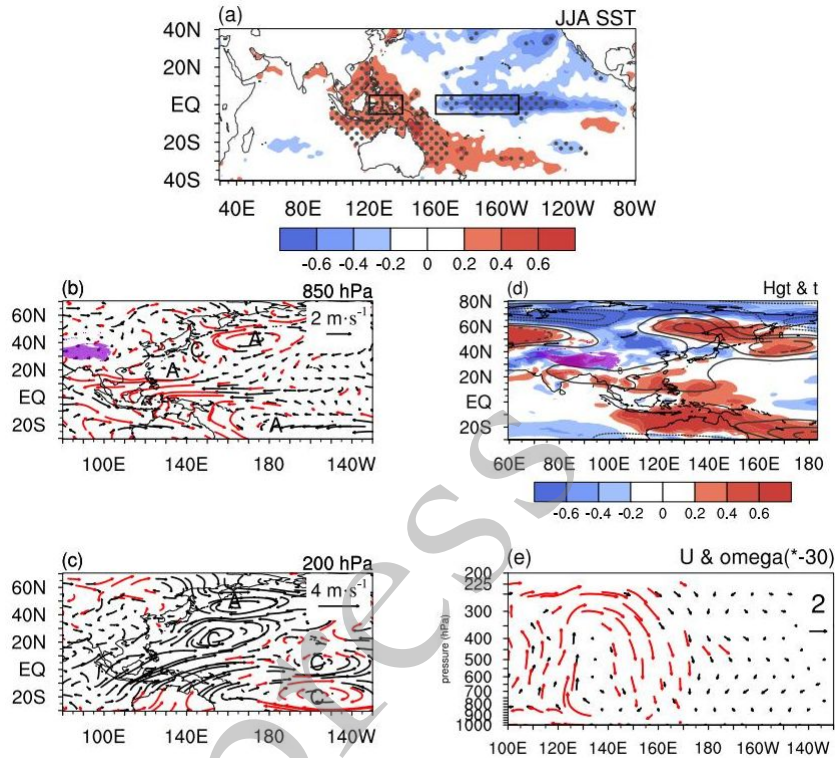


459

460 **FIG. 9.** The difference of sensitive experiment and control experiment when the  
 461 negative SSTA is added in tropical western Pacific and positive SSTA added in Niño 4,  
 462 marked by rectangle in Fig. 8(a) and detailed description shown in section 2. (a)/(b) for  
 463 850 hPa/200 hPa horizontal wind (unit: m s<sup>-1</sup>), the key anomalies are marked by red  
 464 vector.

465

466 Based on 1996, 1998, and 2010 years, we conduct the composite analyses of SST  
 467 and horizontal wind fields to explore the combination effect of the positive SSTA in the  
 468 tropical western Pacific and negative SSTA in Niño 4 area on WNPSM (Fig. 10). As  
 469 shown in Fig. 10a, it is reproduced that SSTA is negative in the Niño 4 area, but  
 470 positive in the tropical western Pacific during 1996, 1998, and 2010 years.



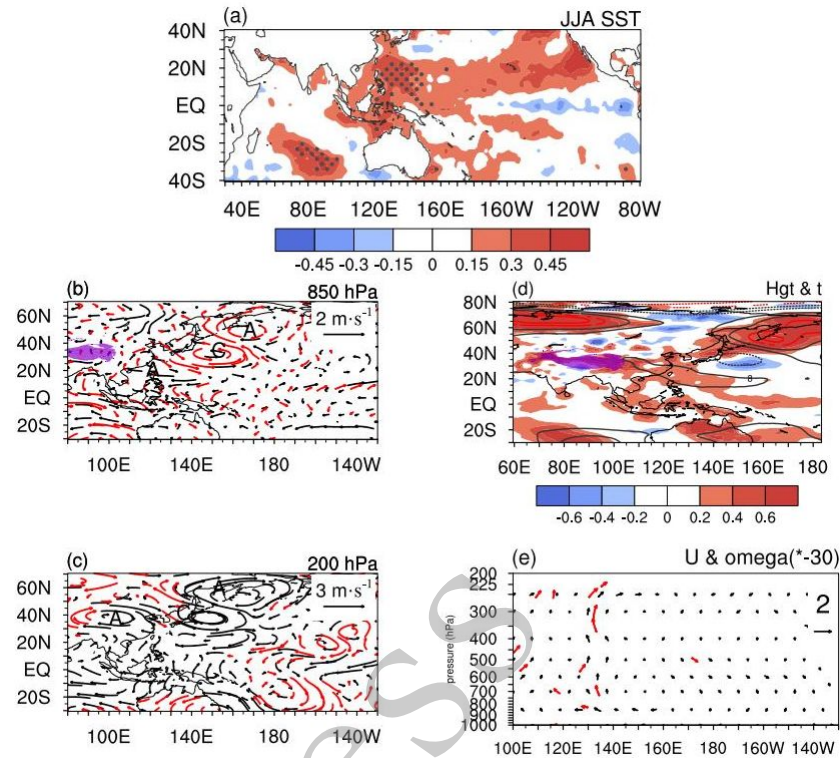
471

472 **FIG. 10.** Same as Fig. 8, but for 1996, 1998, and 2010 year.

473

474 The wind anomalies in Figs. 10b, 10c present a negative phase of PJ-like pattern,  
 475 with the opposite phase to those displayed in Figs. 8b, 8c. Especially, the negative PJ-  
 476 like circulation anomalies at 200 hPa do not pass through 95% confidence level, also  
 477 with the lack of polarity near the equator (Fig. 10c). In terms of the 500-hPa  
 478 geopotential height anomaly and 2-m temperature anomaly, the PJ-like pattern is much  
 479 too weak (Fig. 10d). As shown in Fig. 10e, there exists an anomalous Walker  
 480 circulation between the tropical western Pacific and tropical central Pacific, help to  
 481 maintain the positive SSTA in the tropical western Pacific and negative SSTA in Niño 4  
 482 area. The anomalous years are La Niña developing year, except for 1996 year, so,  
 483 during the La Niña developing year in P2, the SSTA is negative in Niño 4 and positive  
 484 in the tropical western Pacific, both of which can work in coherence to influence

485 WNPSM, showing obvious symmetry, compared to Fig. 8. Because of the prominent  
 486 symmetry, the opposite sensitive experiment to Fig. 9 has no need to carry out.



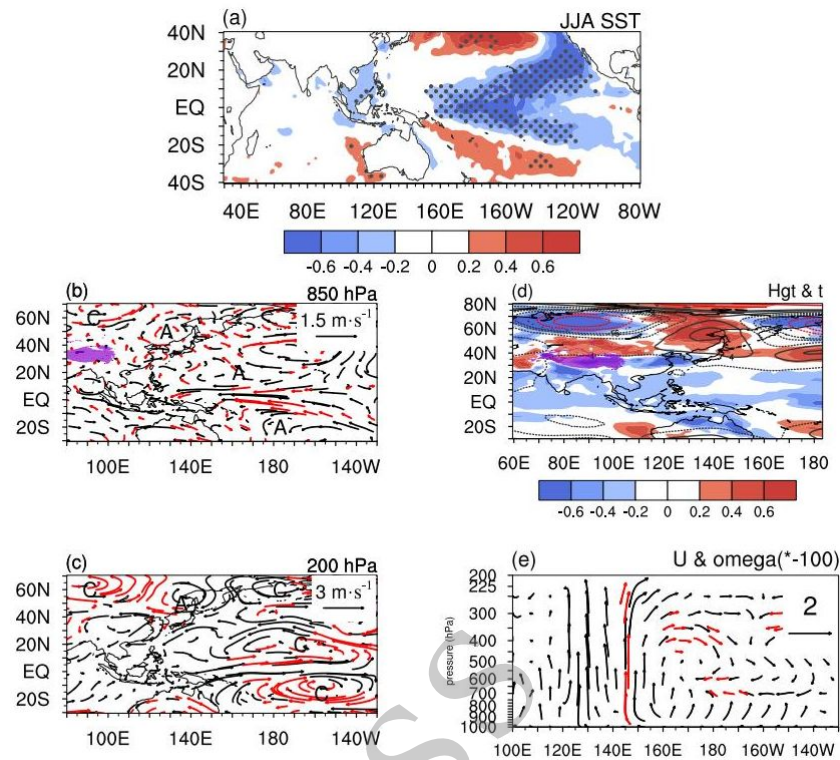
487

488 **FIG. 11.** Same as Fig. 8, but based on 2013, 2014, 2016 and 2017 years.

489

490 As shown in Table 1, 2013, 2014, 2016 and 2017 are positive anomalous years of  
 491 the tropical western Pacific SSTA and Niño 4 normal year, based on these years, to  
 492 conduct composite analyses helps to isolate the independent influence from tropical  
 493 western Pacific on WNPSM. As shown in Fig. 11a, during these years, anomalous  
 494 SSTA in the tropical western Pacific and no significant anomaly over Niño 4 area are  
 495 reproduced. In Fig. 11b, at 850 hPa, also there is a negative phase PJ-like wave, when  
 496 there is positive SSTA in the tropical western Pacific. At 200 hPa, Fig. 11c also  
 497 demonstrate some similarities to Figs. 5e, 7c, but only out of phase. The geopotential  
 498 height and temperature anomalies in Fig. 11d also can reappear the out-of-phase  
 499 circulation pattern anomalies, compared to Fig. 5f. As shown in Fig. 11e, the anomalous  
 500 ascending motion appears in the tropical western Pacific. The analyses about the  
 501 “Positive & Negative” type, namely positive SSTA in the tropical western Pacific and  
 502 normal SSTA in Niño 4, show that tropical SSTA can influence WNPSM by PJ-like  
 503 wave. When the SSTA in tropical western Pacific is positive (negative), a negative  
 504 (positive) phase PJ-like wave appears, and weaken (strengthen) the WNPSM (Figs. 7a–f,

505 10a–e).



506

507 **FIG. 12.** Same as Fig. 8, but based on 1999, 2008, and 2011 years.

508

509 As shown in Table 1, 1999, 2008, and 2011 are normal years of tropical western  
510 Pacific SSTA and negative anomaly of SSTA in Niño 4, based on these years, to  
511 conduct composite analyses helps to isolate the independent influence from Niño 4 on  
512 WNPSM. As shown in Fig. 12a, during these years, negatively anomalous SSTA in  
513 Niño 4 and no significant anomaly over tropical western Pacific are reproduced. In Fig.  
514 12b, at 850 hPa, there is an abnormal anticyclone to the north and south sides of the  
515 equator, respectively and at 200 hPa, they develop into cyclones (Fig. 12c), which  
516 further confirms that the Niño 4 exerts influences on WNPSM by Gill response,  
517 consistent with the results obtained in Fig. 6b–c. The geopotential height and  
518 temperature anomalies in Fig. 12d also present weaker circulation anomalies, compared  
519 to Fig. 6d. At the same time, the anomalous Walker circulation is very weak, with weak  
520 descending motion over Niño 4 area (Fig. 12e). 1999, 2008, 2011 are also CP La Niña  
521 developing years, in which the negative SSTA in Niño 4 area works alone on WNPSM.  
522 When the SSTA in Niño 4 is negative (positive), the abnormal anticyclone (cyclone) in  
523 WNP at 850 hPa can weaken (enhance) the WNPSM (Figs. 6a–f, 12a–e). Besides, there

524 is a BBC-like wave appearing in 40°–80°N, along with the occurrence of Gill response  
525 (Fig. 12b, c), and whether the BBC plays a role in influencing WNPSM or not needs to  
526 further be investigated in future studies.

527 On the whole, during the El Niño (La Niña) developing year in P2, the negative  
528 (positive) SSTA in the tropical western Pacific and positive (negative) SSTA in the  
529 Niño 4 area, could work together to influence WNPSM, enhancing (weakening) the  
530 WNPSM, by the positive (negative) phase PJ-like wave and Gill response. In some  
531 years, the positive SSTA in the tropical western Pacific can work alone to influence  
532 WNPSM in P2, weakening the WNPSM, by the negative phase PJ-like wave. During  
533 CP La Niña developing years, the negative SSTA anomaly in the Niño 4 area can work  
534 alone to exert impact on WNPSM in P2, weakening the WNPSM, by the Gill response  
535 with an anomalous anticyclone in WNP. Both of them further confirm that SSTA in the  
536 tropical western Pacific (Niño 4) exerts influences on WNPSM by PJ-like wave (Gill  
537 response), consistent with the results displayed in section 4.

538

## 539 **6. Summary and Discussion**

540 In view of the analyses above, it could be obtained that the correlation between  
541 WNPSM and SSTA in the tropical Pacific underwent a dramatically interdecadal shift  
542 around the early 1990s, with the enhanced linkage to tropical western Pacific and Niño  
543 4 SSTA during the summertime from P1 to P2. The rainfall and circulation connected  
544 with WNPSM also display similar features, with a significant PJ-like pattern during P1,  
545 and when the influence of Niño 3 in the preceding winter is removed, the PJ-like pattern  
546 disappears. Those imply that Niño 3-related SSTA is the most important factor of  
547 generating influence on WNPSM during P1. During P2, the associated precipitation  
548 shows a zonal dipole pattern, connected with both Niño 4 area and tropical western  
549 Pacific. The SSTA in the Niño 4 area exerts impacts on WNPSM by atmospheric Gill  
550 response, with stronger (weaker) WNPSM along with positive (negative) SSTA in Niño  
551 4 and SSTA associated with the tropical western Pacific exerts influences on WNPSM  
552 by PJ-like wave, with stronger (weaker) WNPSM along with negative (positive) SSTA  
553 in the tropical western Pacific.

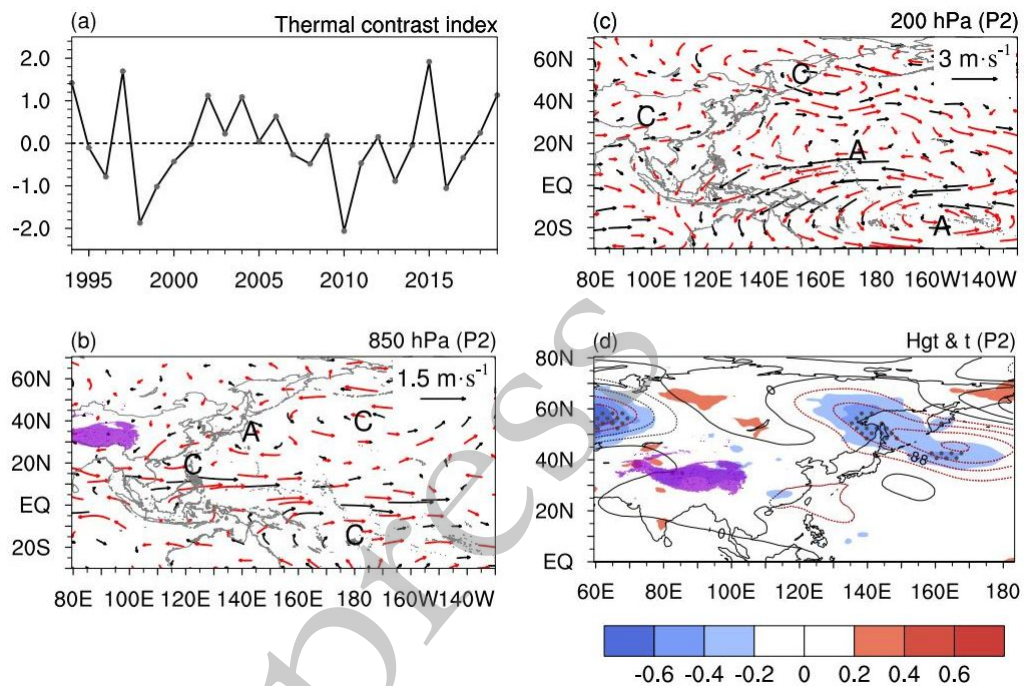
554 In the combination of “Negative & Positive” ( “Positive & Negative”) of TWPI

555 and Niño4, namely during the El Niño (La Niña) developing year in P2, the negative  
556 (positive) SSTA in the tropical western Pacific and positive (negative) SSTA in the  
557 Niño 4 area, could work in accordance to influence WNPSM, enhancing (weakening)  
558 the WNPSM, by the positive (negative) phase PJ-like wave and Gill response, with an  
559 anomalous cyclone (anticyclone) located in WNPSM, which shows obvious symmetry.  
560 During the combination of “Positive & Normal”, the positive SSTA in tropical western  
561 Pacific can work alone to influence WNPSM in P2, weakening the WNPSM, by the  
562 negative phase PJ-like wave. During the combination of “Normal & Positive”, namely  
563 during CP La Niña developing years, the negative SSTA anomaly in Niño 4 area can  
564 work alone to exert impacts on WNPSM in P2, weakening the WNPSM, by the Gill  
565 response with an anomalous anticyclone in WNP. In addition, westerly wind bursts  
566 (WWBs) play an important role in ENSO prediction, through affecting surface zonal  
567 currents and triggering eastward downwelling Kelvin waves (McPhaden et al. 1992;  
568 Lengaigne et al. 2004). In the last several years, using parameterized WWBs could  
569 obviously improve the WWBs representation in coupled models and lead to more  
570 accurately simulation of extreme El Niño and central Pacific El Niño (Tan et al. 2020).  
571 With the improvement of Niño 4 prediction skill, the results obtained in this paper  
572 would have important implications for WNPSM prediction. According to the research  
573 results, it may be necessary to adjust the strategy of the WNPSM prediction according  
574 to the early SST precursor signals in different decades (before and after the 1990s).

575       The interdecadal enhancement of the relationship between WNPSM and SST in the  
576 tropical central-west Pacific from P1 to P2, maybe is linked to the ENSO decadal shift,  
577 with more CP ENSO events in P2, which is more closely related to the enhanced  
578 influences from the Atlantic multidecadal oscillation (AMO) (Yu et al. 2015; Wang et  
579 al. 2017) and the variations of anomalous cyclone/anticyclone in western North Pacific  
580 and atmosphere-ocean interaction related to WPSH (Wang et al. 2003; Huang et al.  
581 2018), both of which maybe have direct or indirect connection with WNPSM. However,  
582 Wu and Wang (2019) argued that the concurrent tropical Atlantic (Indian) ocean SST  
583 anomalies could constructively reinforce (destructively mitigate) the WNPSM  
584 anomalies induced by the summertime Niño 3.4 SST, thus boosting (muting) the  
585 correlation between the summertime Niño 3.4 SST and the WNPSM index after (before)  
586 the early 1990, which maybe is associated with more frequent occurrences of CP El  
587 Niño and the interdecadal changes in ENSO-associated SST anomalies. In addition, the

588 relationship between ENSO and monsoon can be modulated by PDO and IPO. Such as,  
 589 the ENSO has little (strong) effect on monsoonal winds during the warm (cold) PDO  
 590 phase (Wu, 2013); and the IPO negative phase corresponds to a La Niña-like SST  
 591 anomalies, which strengthens the Walker circulation in the tropical Pacific (Zhao et al.  
 592 2018), and maybe exerts influences on WNPSM. These need to be further investigated  
 593 in the future research.

594



595

596 **FIG. 13.** (a) Same as Fig. 6, but for TCWI.

597

598 If use the TCWI instead of Niño 4 and TWPI to study the influence of tropical  
 599 central-western Pacific on WNPSM, we could get the Fig. 13. The circulation anomaly  
 600 in Fig. 13b is more same as that in Fig. 7b, but the anomalous pattern in Fig. 13c is  
 601 more similar to that in Fig. 6c. As shown in Fig. 13d, the anomalous circulations in 500  
 602 geopotential height and 2-m temperature are more similar to Fig. 6d, compared to Fig.  
 603 7d. To use TCWI to study the influence of tropical central-western Pacific on WNPSM  
 604 can not distinguish the relative contribution of Niño 4 and tropical western Pacific to  
 605 WNPSM. So, in the paper, we use Niño 4 and TWPI, but not TCWI, to study the  
 606 interdecadal enhancement in the relationship between WNPSM and SSTA in the  
 607 tropical central-western Pacific. In addition, the reanalysis data used in the paper is  
 608 replaced by NCEP or EAR-40, the results are also robust.

610 **Acknowledgments.** We cordially thank all the dataset providers. This work is  
611 supported by the Fund Project of the Hengyang Normal University (2022QD11) and  
612 National Key Research and Development Program of China (2016YFA0600603) and  
613 the National Natural Science Foundation of China (grant no. 42105063).

614

#### 615 **Data Availability Statement**

616 The JRA-55 monthly reanalysis data is freely available at  
617 <http://jra.kishou.go.jp/JRA-55/>. The GPCP data is available at  
618 <https://psl.noaa.gov/data/gridded/data.gpcp.html>. The HadISST data is available at  
619 <https://www.metoffice.gov.uk/hadobs/hadisst/>. The Community Atmospheric Model of  
620 version 5.0 can be downloaded at <https://www.cesm.ucar.edu/models/cesm1.1/>. The  
621 analysis scripts are available upon request from the corresponding author.

622

in press

- 625 Adler, R. F., and Coauthors, 2003: The version2 global precipitation climatology  
626 project (GPCP) monthly precipitation analysis (1979 present). *J.*  
627 *Hydrometeorol.*, **4(6)**, 1147-1167.
- 628 Briegel, L. M., and W. M. Frank, 1997: Large-scale influences on tropical cyclogenesis  
629 in the western North Pacific. *Mon. Wea. Rev.*, **125**, 1397-1413, doi:10.1175/1520-  
630 0493(1997)125,1397:LSIOTC.2.0.CO;2.
- 631 Cao, X., T. Li, M. Peng, W. Chen, and G. Chen, 2014: Effects of monsoon trough  
632 interannual variation on tropical cyclogenesis over the western North Pacific.  
633 *Geophys. Res. Lett.*, **41**, 4332-4339, doi:10.1002/2014GL060307.
- 634 Choi, K. S., Y. Cha, H. D. Kim, and S. D. Kang, 2016: Possible influence of western  
635 North Pacific monsoon on TC activity in mid-latitudes of East Asia. *Climate Dyn.*,  
636 **46**, 1-13, <https://doi.org/10.1007/s00382-015-2562-9>.
- 637 Chou, C., J. Tu, and J. Yu, 2003: Interannual variability of the western north pacific  
638 summer monsoon: differences between enso and non-ENSO years. *J.*  
639 *Climate*, **16(13)**, 2275-2287.
- 640 Feng, X., and L. Wu, 2021: Roles of interdecadal variability of the western North  
641 Pacific monsoon trough in shifting tropical cyclone formation. *Climate Dyn.*, 1-9.  
642 <https://doi.org/10.1007/s00382-021-05891-w>.
- 643 Fu, C., and D. Ye, 1988: The tropical very Low-frequency Oscillation on interannual  
644 scale. *Adv. Atmos. Sci.*, **5**, 369-388.
- 645 Gray, W. M., 1968: Global view of the origin of tropical disturbances and storms. *Mon.*  
646 *Wea. Rev.*, **96**, 669-700, doi:10.1175/1520-  
647 0493(1968)096,0669:GVOTOO.2.0.CO;2.
- 648 Guan, B., and J. C. Chan, 2006: Nonstationarity of the intraseasonal oscillations  
649 associated with the western North Pacific summer monsoon. *J. Climate*, **19**, 622-629,  
650 <https://doi.org/10.1175/JCLI3661.1>.
- 651 He, B., Y. Zhang, T. Li, and W. T. Hu, 2017: Interannual variability in the onset of the  
652 South China Sea summer monsoon from 1997 to 2014. *Atmos. Oceanic Sci. Lett.*, **10**,  
653 73-81, <https://doi.org/10.1080/16742834.2017.1237853>.
- 654 Hu, K., and S.-M., Long, 2020: The optimal heat source for interannual variability of  
655 the Western North Pacific summer monsoon, *Atmos. Oceanic Sci. Lett.*, **13(1)**, 41-47,  
656 <https://doi.org/10.1080/16742834.2019.1680087>.

657 Huang, Y., B. Wang, X. Li, and H. Wang, 2018: Changes in the influence of the  
658 western Pacific subtropical high on Asian summer monsoon rainfall in the late  
659 1990s. *Climate Dynamics*, **51(1)**, 443-455.

660 Janowiak, J. E., and P. Xie, 2003: A global-scale examination of monsoon-related  
661 precipitation. *J. Climate*, **16(24)**, 4121-4133.

662 Kobayashi, S., Y. Ota, Y. Harada, A. Ebita, M. Moriya, H. Onoda, K. Onogi, H.  
663 Kamahori, C. Kobayashi, H. Endo, K. Miyaoka, and K. Takahashi, 2015: The JRA-  
664 55 reanalysis: general specifications and basic characteristics. *J. Meteor. Soc. Japan*,  
665 **93**, 5-48.

666 Kosaka, Y., and H. Nakamura, 2010: Mechanisms of meridional teleconnection  
667 observed between a summer monsoon system and a subtropical anticyclone. Part I:  
668 The Pacific–Japan pattern. *J. Climate*, **23**, 5085-5108.

669 Kwon, M., J. G. Jhun, B. Wang, S. I. An, and J. S. Kug, 2005: Decadal change in  
670 relationship between east Asian and WNP summer monsoons. *Geophysical research*  
671 *letters*, **32(16)**, L16709, <https://doi.org/10.1029/2005GL023026>.

672 Lee, E. J., K. J. Ha, and J. G. Jhun, 2014: Interdecadal changes in interannual  
673 variability of the global monsoon precipitation and interrelationships among its  
674 subcomponents. *Climate Dyn.*, **42(9-10)**, 2585-2601,  
675 <https://doi.org/10.1007/s00382-013-1762-4>.

676 Lengaigne, M., J. P. Boulanger, C. Menkes, P. Delecluse, and J. Slingo, 2004: Westerly  
677 wind events in the tropical pacific and their influence on the coupled ocean-  
678 atmosphere system: A review. *Geophysical Monograph Series*, **147**, 49-69.  
679 <https://doi.org/10.1029/147GM03>.

680 Li, T., and B. Wang, 2005: A review on the western North Pacific monsoon: Synoptic-  
681 to-interannual variabilities. *Terr. Atmospheric Ocean. Sci.*, **16**, 285-314,  
682 [https://doi.org/10.3319/TAO.2005.16.2.285\(A\)](https://doi.org/10.3319/TAO.2005.16.2.285(A)).

683 McPhaden, M. J., F. Bahr, Y. Du Penhoat, E. Firing, S. P. Hayes, P. P. Niiler, et al.  
684 1992: The response of the western equatorial Pacific Ocean to westerly wind bursts  
685 during November 1989 to January 1990. *Journal of Geophysical Research:*  
686 *Oceans*, **97(C9)**, 14289-14303.

687 Molinari, J., and D. Vollaro, 2013: What percentage of western North Pacific tropical  
688 cyclones form within the monsoon trough? *Mon. Wea. Rev.*, **141**, 499-505,  
689 doi:10.1175/MWR-D-12-00165.1.

690 Neale, R. B., and Coauthors, 2010: Description of the NCAR community atmosphere  
691 model (CAM 5.0). NCAR Tech. Note NCAR/TN-4861 STR, 274 pp.

692 Rayner, N. A., D. E. Parker, E. B. Horton, C. K. Folland, L. V. Alexander, D. P. Rowell,  
693 E. C. Kent, and A. Kaplan, 2003: Global analyses of sea surface temperature, sea ice,  
694 and night marine air temperature since the late nineteenth century. *J Geophys. Res.*,  
695 **108 (D14)**, doi 10.1029/2002JD002670.

696 Tan, X., Y. Tang, T. Lian, S. Zhang, T. Liu, and D. Chen, 2020: Effects of  
697 semistochastic westerly wind bursts on ENSO predictability. *Geophysical Research*  
698 *Letters*, 47(14), e2019GL086828.

699 Vega, I., P. Ribera, and D. Gallego, 2020: Characteristics of the onset, withdrawal, and  
700 breaks of the western north pacific summer monsoon in the 1949–2014 period. *J.*  
701 *Climate*, **33(17)**, 7371-7389.

702 Wang, B., R. Wu, and X. Fu, 2000: Pacific–East Asia teleconnection: How does ENSO  
703 affect East Asian climate? *J. Climate*, **13**, 1517-1536.

704 Wang, B., R. G. Wu, and K. M. Lau, 2001: Interannual variability of the Asian summer  
705 monsoon: Contrasts between the Indian and the western North Pacific-East Asian  
706 monsoons. *J. Climate*, **14**, 4073-4090.

707 Wang, B., and Z. Fan, 1999: Choice of South Asian summer monsoon indices. *Bull.*  
708 *Amer. Meteor. Soc.*, **80**, 629-638.

709 Wang, B., and X. Xu, 1997: Northern Hemisphere summer monsoon singularities and  
710 climatological intraseasonal oscillation. *J. Climate*, **10(5)**, 1071-1085.

711 Wang, B., 2002: Rainy season of the Asian–Pacific summer monsoon. *J. Climate*, **15(4)**, 386-  
712 398.

713 Wang, B., R. Wu, and T Li, 2003: *Atmosphere – warm ocean interaction and its*  
714 *impacts on Asian – Australian monsoon variation. Journal of Climate*, 16(8), 1195-  
715 1211.

716 Wang, L., J. Y. Yu, and H. Paek, 2017: Enhanced biennial variability in the Pacific due  
717 to Atlantic capacitor effect. *Nat. Commun.*, **8(1)**, 1-7.

718 Wang, L., and J. Y. Yu, 2018: A recent shift in the monsoon centers associated with the  
719 tropospheric biennial oscillation. *J. Climate*, **31(1)**, 325-340,  
720 <https://doi.org/10.1175/JCLI-D-17-0349.1>.

721 Wu, C. R. 2013: *Interannual modulation of the Pacific Decadal Oscillation (PDO) on*  
722 *the low-latitude western North Pacific. Progress in Oceanography*, **110**, 49-58.

723 Wu, L., Z. Wen, R. Huang, and R. Wu, 2012: Possible linkage between the monsoon

724 trough variability and the tropical cyclone activity over the western North Pacific.  
725 *Mon. Wea. Rev.*, **140**, 140-150, doi:10.1175/MWR-D-11-00078.1.

726 Wu, M., and L. Wang, 2019: Enhanced correlation between ENSO and western North  
727 Pacific monsoon during boreal summer around the 1990s. *Atmos. Ocean. Sci. Lett.*,  
728 *12*(5), 376-384, <https://doi.org/10.1080/16742834.2019.1641397>.

729 Wu, R., and B. Wang, 2000: Interannual variability of summer monsoon onset over the  
730 western North Pacific and the underlying processes. *J. Climate*, **13**(14), 2483-2501,  
731 <https://doi.org/10.1175/1520-0442>.

732 Wu, R., 2002: Processes for the northeastward advance of the summer monsoon over  
733 the western North Pacific. *J. Meteor. Soc. Japan, Ser. II*, **80**(1), 67-83.  
734 <https://doi.org/10.2151/jmsj.80.67>.

735 Xu, K., and R. Lu, 2018: Decadal change of the western North Pacific summer  
736 monsoon break around 2002/03. *J. Climate*, **31**, 177-193.

737 Xu, K., and R. Lu, 2015: Break of the western North Pacific summer monsoon in early  
738 August. *J. Climate*, **28**, 3420-3434.

739 Xie, S. P., K. M. Hu, J. Hafner, H. Tokinaga, Y. Du, G. Huang, and T. Sampe, 2009:  
740 Indian Ocean Capacitor Effect on Indo-Western Pacific Climate during the Summer  
741 following El Niño. *J. Climate*, **22**, 730-747.

742 Xie, Y., Q. Huang, J. Chang, S. Liu, and Y. Wang, 2016: Period analysis of hydrologic  
743 series through moving-window correlation analysis method. *Journal of*  
744 *Hydrology*, *538*, 278-292.

745 Xu, K., and R. Lu, 2016: Change in tropical cyclone activity during the break of the  
746 western North Pacific summer monsoon in early August. *J. Climate*, **29**, 2457-2469.

747 Xu, P., L. Wang, and W. Chen. 2019: The British–Baikal corridor: A teleconnection  
748 pattern along the summertime polar front jet over Eurasia. *J. Climate*, **32**(3), 877-  
749 896.

750 Yim, S.-Y., J.-G. Jhun, and S.-W. Yeh, 2008: Decadal change in the relationship  
751 between east Asian-western North Pacific summer monsoons and ENSO in the mid-  
752 1990s. *Geophys. Res. Lett.*, **35**, L20711, doi:10.1029/2008GL035751.

753 Yu, J.-Y., P.-K. Kao, H. Paek, H.-H. Hsu, C.-W. Hung, M.-M. Lu, and S.-  
754 I. An, 2015: Linking emergence of the central Pacific El Niño to the Atlantic Multi-  
755 decadal Oscillation. *J. Climate*, *28*, 651–662, [https://doi.org/10.1175/JCLI-D-14-](https://doi.org/10.1175/JCLI-D-14-00347.1)  
756 [00347.1](https://doi.org/10.1175/JCLI-D-14-00347.1).

757 Zhang, R., A. Sumi, and M. Kimoto, 1996: Impact of El Niño on the East Asian  
758 Monsoon: A Diagnostic Study of the '86/87 and '91/92 Events. *Journal of the*  
759 *Meteorological Society of Japan*, **74**, 49-62.

760 Zhao, J., R. Zhan, Y. Wang, and H. Xu, 2018: Contribution of the interdecadal Pacific  
761 oscillation to the recent abrupt decrease in tropical cyclone genesis frequency over  
762 the western North Pacific since 1998. *J. Climate*, **31**(20), 8211-8224.

763 Zhao, H., S. Chen, and P. J. Klotzbach, 2019: Recent strengthening of the relationship  
764 between the Western North Pacific monsoon and Western North Pacific tropical  
765 cyclone activity during the Boreal summer. *J. Climate*, **32**, 8283-8299,  
766 doi:10.1175/JCLI-D-19-0016.1.

767 Zeng, X., and E. Lu, 2004: Globally unified monsoon onset and retreat indexes. *J.*  
768 *Climate*, **17**(11), 2241-2248.

769 Zong, H., and L. Wu, 2015: Re-examination of tropical cyclone formation in monsoon  
770 troughs over the western North Pacific. *Adv. Atmos. Sci.*, **32**, 924-934,  
771 doi:10.1007/s00376-014-4115-2.

772 Zhou, W., and J.C.L. Chan, 2007: ENSO and South China Sea summer monsoon  
773 onset. *International Journal of Climatology*, **27**, 157-167.

774 Zhou, W., and J.C.L. Chan, 2005: Intraseasonal oscillations and the South China Sea  
775 summer monsoon onset. *International Journal of Climatology*, **25**, 1585-1609.